Original article
https://doi.org/10.18019/1028-4427-2025-31-3-350-360

Biocompatibility and osteointegrative characteristics of zirconium ceramic implants for diaphyseal defect filling

E.A. Volokitina[1]✉, M.V. Saushkin[1], I.P. Antropova[1], S.M. Kutepov[1], S.A. Brilliant[2]

[1] Urals State Medical University, Ekaterinburg, Russian Federation

[2] Institute of Immunology and Physiology Ural Branch of the Russian Academy of Sciences, Ekaterinburg, Russian Federation

Corresponding author: Elena A. Volokitina, volokitina_elena@rambler.ru

Abstract

Introduction The development of new ceramic materials with high osteointegrative characteristics and experimental substantiation of their application is an important issue in traumatology. The purpose of the work was to study the biological compatibility and osteointegrative characteristics of implants made of zirconium ceramics stabilized with yttrium, ytterbium and gadolinium for filling diaphyseal bone defects in an experiment.

Material and methods The study was performed on 18 male Chinchilla rabbits. Diaphyseal defects with intramedullary implantation of a rod made of a new ceramic porous (PC), non-porous (NPC) material and titanium alloy (TA) were modelled. The animals were divided into 3 groups based on the rod used: PC, NPC and TA (n = 6 in each). Hematological parameters were studied one day before and 8 weeks after the operation. Withdrawal of animals from the experiment, X-ray control and tissue sampling with subsequent histological and morphometric examination were performed at 8 weeks after the operation. Statistical data processing was performed using the Statistica 10 software. The Kruskal – Wallis test with subsequent intergroup analysis was used to compare the study groups. The Wilcoxon criterion was used to assess changes in dynamics in individual groups. The results are presented as median and interquartile range.

Results Eight weeks after the surgery, in the PC group compared to the NPC and TA groups the levels of leukocytes, monocytes and granulocytes were significantly lower (p = 0.025; p = 0.022; p = 0.005, respectively); no significant differences were found in other hematological parameters. The results of histomorphological studies showed that better integration of implants was observed when using PC rods compared to TA and NPC implants. The thickness of the bone trabecula in the implantation area was significantly higher in the PC group compared to the TA and NPC groups (86.2 [55.8; 109.9], 56.0 [47.2; 75.9] and 33.1 [19.0; 84.5], respectively, in both cases p < 0.001).

Discussion We studied the biocompatibility and osteointegrative properties of implants made of a new ceramic material in two versions, nonporous and porous (pore size of 10–50 μm), and compared them with titanium alloy implants. It was previously proven that alloyed ceramic materials are attractive for tissue regeneration due to their functional properties, biological activity, and therapeutic effects provided by the introduced ions. The results of our histological and morphometric studies confirmed the better biocompatibility and osteointegration of implants made of porous zirconium ceramics (PC) containing yttrium, ytterbium, and gadolinium ions, compared to implants made of NPC and TA.

Conclusion A new zirconium-based ceramic demonstrates biological compatibility. Implants with pore sizes of 10–50 μm have good osteointegrative characteristics which determine their possible use in the treatment of bone defects.

Keywords: diaphysis, bone defect, implant, zirconium ceramics, biological compatibility, osseointegration, experiment

For citation: Volokitina EA, Saushkin MV, Antropova IP, Kutepov SM, Brilliant SA. Biocompatibility and osteointegrative characteristics of zirconium ceramic implants for diaphyseal defect filling. *Genij Ortopedii*. 2025;31(3):350-360. doi: 10.18019/1028-4427-2025-31-3-350-360.

INTRODUCTION

In 2020, in peacetime, more than 11 million fractures resulting from accidents were registered in Russia. Bone injuries to the upper limbs in the structure of injuries, poisoning and other consequences of external causes amounted to 34.6 %, the lower limbs to 33.2 %, malignant neoplasms of bone tissue to 4.2 % of all oncological diseases [1]. The rate of limb injuries during military conflicts of the last decade exceeds 60–70 % and does not tend to decrease, while injuries to the lower limbs with disruption of bone integrity and weight-bearing function occur twice as often as to the upper limbs [2]. The presence of a bone defect is the cause of long-term, sometimes failed treatment, and can lead to persistent disability [3]. To compensate diaphyseal defects, various methods of auto- and alloplasty are used in combination with closed intramedullary osteosynthesis with a titanium nail or transosseous distraction osteosynthesis, as well as a combination of bone grafting technologies according to Ilizarov and Masquelet [4].

An orthopedic traumatologist must have a sufficient number of implants/augmentations of various designs, as well as a diverse arsenal of osteoplastic and bone substituting materials to treat a pathological orthopedic symptom complex and critical bone tissue defects resulting from high-energy and gunshot trauma. Autobone, allografts and demineralized matrix as bone substituting materials are often not applicable for extensive defects; there are risks of donor bed inflammation, immune reaction of recipients and rejection of a foreign implant [5]. Special bioinert durable materials and structures made of ceramics and titanium with high osteointegrative characteristics are required, which will allow not only recovery of the shape of the lost bone fragment, but also restoration of the supporting function of the limb as a whole [6, 7].

The use of artificial bone substitute biomaterials has advantages due to their compatibility with autologous bone, ease of modeling and the possibility of their use in large volumes [8]. Bioceramics have found wide application in surgical traumatology and orthopedics [6]. In Russia and abroad, various types of ceramics based on calcium phosphate are successfully used, being the closest materials in their composition and structure to human bone tissue [9], as well as zirconium ceramics due to their inertness to body tissues and good mechanical characteristics [10]. Moreover, a positive effect of zirconium on osteoblasts has been shown [11]. Research has been conducted on the modification of the chemical structure of bone substituting materials to optimize their biointegration and physical characteristics [12]. In particular, the introduction of rare earth elements into zirconium ceramics has a significant effect on the corrosion resistance of composites [13] and on the inhibition of the expression of genes specific to osteoclasts [14].

Due to the fact that the development of new ceramic materials with high osteointegrative features and experimental trials of their use for diaphyseal defects is a relevant problem in modern traumatology, the Mikroakustika LLC has developed a new ceramic material, zirconium ceramics stabilized with yttrium, ytterbium and gadolinium Zr9Y5Yb5Gd (TU-20.12.19.001-20883295-2020). The ceramic material has corrosion and erosion resistance, wear resistance, is resistant to oxidation and high-temperature sterilization.

The **purpose** of the work was to study the biological compatibility and osteointegrative characteristics of implants made of zirconium ceramics stabilized with yttrium, ytterbium and gadolinium for filling diaphyseal bone defects in experimental conditions.

MATERIALS AND METHODS

Samples for tests

A new ceramic material was studied: zirconium ceramics stabilized with yttrium, ytterbium and gadolinium. The samples were made by cold pressing followed by sintering in an atmospheric furnace. After sintering, final mechanical treatment was performed. Samples of the ceramic material of two types were prepared: non-porous and porous (pore size 10–50 μm). Rods for fracture osteosynthesis (intramedullary implantation) 50 mm long with a round cross-section of 5 mm were fabricated from porous and non-porous materials. Rods of a similar size were made of a medical titanium-based alloy.

Experimental animals

The study was performed on 18 male Chinchilla rabbits weighing 3–3.5 kg. The animals were kept in identical feeding and housing conditions (at the vivarium of the Ural State Medical University). All animals had a veterinary certificate of quality and health. The protocol for the use and care of animals complied with the "Methodological recommendations for the maintenance of laboratory animals in vivariums of research institutes and educational institutions" RD-APK 3.10.07.02-09 and "Directive 2010/63/EU of the European Parliament and of the Council of the European Union on the protection of animals". The study was approved by the local ethics board of the Ural State Medical University, protocol dated 05.20.2020 No. 5.

Diaphyseal defect modelling and intramedullary implantation of the rod

All animals underwent bilateral modeling of the diaphyseal defect of the femurs and bilateral intramedullary osteosynthesis with rods. In accordance with the study design, the animals were divided into three groups (six in each). Non-porous ceramic (NPC) rods were implanted into the right and left femurs in the first group, porous ceramic rods (PC) were implanted in the second group, and titanium alloy (TA) rods were implanted in the third group.

Under intravenous anesthesia, the medullary canal of the femur in the intercondylar region was retrogradely drilled, and a rod made of bone substituting material was installed in the canal. Then, a linear incision of the skin and fascia was made along the lateral surface of the thigh, and access to the diaphysis of the femur was achieved layer by layer between the muscles. At the border of the middle and lower thirds of the femur, a cylindrical 10-mm long bone defect of the diaphysis was formed by double circular osteotomy which was crossed with a rod made of bone substituting materials that had been retrogradely installed in the medullary canal at the first stage of the surgical intervention. The wound was sutured layer by layer. The animals were withdrawn from the experiment; radiography of the hind limbs and tissue harvesting were performed eight weeks after the operation.

Hematological study

Blood samples were collected from the marginal vein of the rabbits' ears into standard laboratory test tubes one day before surgery and eight weeks after surgery before the animals were withdrawn from the experiment. Hematological parameters were determined using an automatic hematological analyzer Cell-70 (Biocode-Hygel, France). The study was performed according to the protocol recommended by the manufacturer.

Histological study of peri-implant bone tissue

Each sample of laboratory animal femurs, cleared of soft tissue, was fixed by immersion in 10 % buffered formaldehyde at room temperature for at least seven days. After fixation, the samples were decalcified for 48 hours in a solution of hydrochloric (11.5 ± 0.5 %) and formic (5.8 ± 0.3 %) acids, which was changed every 24 hours. Decalcified samples with partially dissolved and removed ceramic specimens, as well as with removed titanium implants, were cut to form two 2- to 4-mm-thick plates at the diaphysis level. The resulting plates were dehydrated in graded ethanol and embedded in paraffin to form blocks. Paraffin blocks were sectioned to a thickness of 3 to 4 μm, and the material was stained with hematoxylin and eosin. Histological and morphometric studies were performed using an Olympus CX-41 microscope and a Levenhuk M1000 PLUS camera. Measurements were taken using the Phenix Phmias 3.0.6731 software. Histomorphological determination of bone trabecular thickness was performed in the peri-implant area (10 measurements per sample, 60 measurements per study group). The length of the bone trabecular surface (LBTS) formed in the implant area, the total length of the osteoblast surface (TLObS) and the total length of the osteoclast surface (TLOcS) located on the surface of these trabeculae were measured in micrometers (μm) on digital images of histological preparations captured at a total magnification of 400× (eyepiece — 10×, lens — 40×). Measurements were taken in at least 20 fields of view for one case. Next, we calculated relative indicators: the percentage of the length of each of the designated cell types. The length of the trabecula was taken as 100 %. The calculation was carried out using the formulas:

%TLObS = TLObS (μm) × 100 % / LBTS(μm);

%TLOcS = TLOcS (μm) × 100 % / LBTS (μm).

Statistical processing of the findings was performed using the methods of variation statistics in Statistica 10. The Kruskal – Wallis test with subsequent intergroup analysis was used to compare the study groups. To assess changes in dynamics (before surgery and eight weeks after surgery) in the groups, the Wilcoxon test for comparing two related (dependent) samples was used. The level of $p < 0.05$ was considered significant. The data are presented as median [interquartile range].

RESULTS

Eight weeks after the implantation of the test materials, radiography of the pelvis and both hind limbs of the experimental animals was taken (Fig. 1). Radiography showed that the area of the diaphyseal defect was bridged by a ceramic implant installed intramedullary and tightly fitted the bone tissue in certain areas. Osteotomy lines were not traced, the cortical plates in the area of the previously formed bone defect were closed. The integrity of the femur was restored.

Fig. 1 Frontal X-ray of the pelvis and both hind limbs of a rabbit with implanted ceramic rods (porous ceramics) eight weeks after surgery

Results of hematological counts of rabbits' blood samples before surgery and eight weeks after surgery are presented in Table 1. Before surgery, no significant differences were found between the groups in any of the studied indicators.

Eight weeks after the surgery, the level of leukocytes, monocytes and granulocytes was significantly lower in the PC group. It was noted that in the NPC group two months after the surgery the level of leukocytes and granulocytes demonstrated a significant increase relative to the initial level while in the PC group a significant decrease in these indicators was observed. No significant differences were found between the groups in the level of lymphocytes, although there was a tendency towards lower values in the PC group for this indicator. No significant differences were found between the studied groups in the number of erythrocytes, hemoglobin level, and volume of erythrocytes. No significant differences were found between the groups in the platelet count of the blood either. At the same time, a significant increase in the number of platelets and plateletcrit relative to the initial level was observed in the TA and NPC groups, which was apparently due to moderate reactive thrombocytosis. In the PC group, the number of platelets did not differ from the preoperative level.

Table 1

Hematological parameters of rabbits before and after surgery

Parameter	Term	Hematological indicators in the studied groups			
		Titanium (TA)	Non-porous ceramics (NPC)	Porous ceramics (PC)	*p*1
Leucocytes, $\times 10^9$/l	1	9.4 [8.0; 11.1]	9.9 [8.0; 10.7]	9.4 [8.0; 12.4]	0.932
	2	11.8 [10.2; 13.00]	11.7 [11.1; 12.4]	7.6 [6.9; 8.1]	**0.021**
*p*2		0.138	**0.028**	**0.028**	
Lymphocytes, $\times 10^9$/l	1	5.3 [4.8; 5.6]	5.7 [5.1; 7.1]	4.9 [4.1; 6.5]	0.301
	2	6.8 [6.3; 8.3]	6.60[5.9; 6.8]	4.6 [4.5; 7.2]	0.103
*p*2		**0.043**	0.686	0.675	
Monocytes, $\times 10^9$/l	1	0.3 [0.2; 0.3]	0.3 [0.2; 0.3]	0.3 [0.2; 0.4]	0.888
	2	0.4 [0.2; 0.5]	0.3 [0.3; 0.3]	0.2 [0.2; 0.2]	**0.043**
*p*2		0.361	0.068	0.285	
Granulocytes, $\times 10^9$/l	1	3.8 [3.0; 5.4]	4.0 [2.8; 3.5]	4.7 [3.9; 5.4]	0.243
	2	4.2 [4.0; 4.7]	5.2 [4.2; 5.4]	2.7 [2.4; 3.4]	**0.005**
*p*2		0.686	**0.028**	**0.028**	
Erythrocytes, $\times 10^{12}$/l	1	6.68 [6.39; 6.93]	6.90 [6.69; 7.17]	6.67 [6.42; 6.78]	0.368
	2	6.83 [6.75; 7.69]	6.82 [6.55; 7.05]	6.94 [6.52; 7.74]	0.816
*p*2		0.345	0.463	0.345	
Hemoglobin, g/l	1	144 [142; 148]	147 [144; 150]	145 [140; 148]	0.526
	2	150 [141; 152]	146 [134; 149]	148 [147; 152]	0.684
*p*2		0.686	0.295	0.281	
Hematocrit, %	1	41.8 [40.5; 41.9]	42.4 [41.3; 42.8]	41.3 [40.9; 42.8]	0.613
	2	43.7 [43.2; 44.0]	42.5 [41.0; 43.6]	42.9 [41.6; 43.1]	0.459
*p*2		0.225	0.917	0.116	
MPV, fl	1	63.2 [62.7; 63.6]	63.2 [61.9; 66.4]	63.3 [62.5; 63.8]	0.927
	2	63.1 [62.4; 64.0]	62.1 [61.0; 62.6]	63.2 [61.2; 64.0]	0.479
*p*2		0.178	0.116	0.463	
Thrombocytes, $\times 10^9$/L	1	372 [341; 429]	491 [473; 575]	429 [392; 508]	0.150
	2	647 [433; 700]	636 [473; 836]	496 [393; 593]	0.264
*p*2		**0.043**	**0.046**	0.249	
MPV, fl	1	5.2 [4.8; 5.5]	5.5 [5.1; 6.0]	5.5 [5.2; 5.8]	0.498
	2	5.1 [5.1; 5.4]	5.3 [4.9; 6.0]	5.2 [5.0; 5.9]	0.963
*p*2		0.500	0.465	0.753	
Plateletcrit, %	1	0.19 [0.18; 0.24]	0.27 [0.23; 0.35]	0.24 [0.22; 0.25]	0.095
	2	0.32 [0.23; 0.36]	0.32 [0.28; 0.50]	0.29 [0.21; 0.30]	0.610
*p*2		**0.043**	**0.028**	0.249	

Note: 1 — before surgery; 2 — eight weeks after surgery; *p*1 — Kruskal – Wallis test; *p*2 — Wilcoxon test

Histomorphometric evaluation of osteointegrative features of implants

Osseointegration studies in the TA group showed that a continuous band of trabecular bone, represented by both lamellar and reticulofibrous bone tissue, was formed around the implant (Fig. 2 a). Active and resting osteoblasts were visualized on the internal side of the trabeculae facing the implant (Fig. 2 c). In some small areas. loose fibrous connective tissue with moderately dilated microvessels filled with erythrocytes was found (Fig. 2 b). Particles of implantation material measuring from one to 7 μm and isolated areas with an increased accumulation of monocyte-macrophage differon cells with signs of phagocytosis were visualized (Fig. 2 c). Local inflammatory infiltrates were detected. A few resorption cavities with osteoclasts were found on the surface of the bone tissue; active osteogenesis and osteoblasts with amorphous bone substance around them were noted in some cavities. Hematopoietic fatty bone marrow occupied a significant place between the bone layer around the implant and the compact plate. The microcirculatory bed in the bone marrow area was represented mainly by dilated thin-walled sinusoidal capillaries with signs of erythrostasis. Moderate reactive changes were noted in the compact plate. It was characterized by thickening of the adhesion lines. expansion of the Haversian canals of osteons (Fig. 2 a). In most Haversian and Volkmann canals, blood microvessels with dilated lumens surrounded by a layer of loose fibrous connective tissue were found (Fig. 2 d). Small layers of partially compacted spongy bone substance were determined on the endosteal and periosteal surfaces of the plate. Vascularized loose connective tissue was found in the intertrabecular spaces (Fig. 2 a). Osteoclastic resorption was weak. There were signs of reactive reparative restructuring of the maternal bone against the background of sluggish chronic aseptic inflammation due to mild metallosis in the peri-implant zone. The relative extent of the osteoblast surface was 57.47 %, the relative extent of the osteoclast surface was 4.5 %. In general, osseointegration of the implant was noted, the material used did not cause a pronounced negative impact on the tissues of the compact plate and bone marrow.

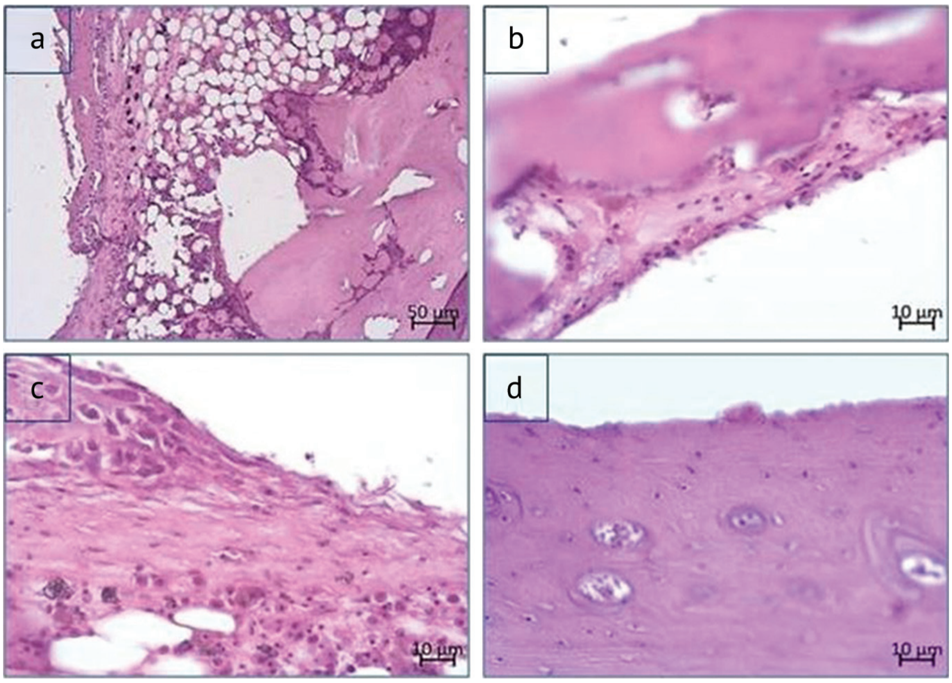

Fig. 2 Histological structure of tissues in the area of TA implantation: (a) formation of a bone "sleeve" of trabecular structure around the implant; (b) fibrous connective tissue on the surface of the trabecular bone on the side adjacent to the implant, osteoclasts are visible on the surface of the bone trabeculae; (c) area of loose fibrous connective tissue in the intertrabecular zone with signs of imbibition of the implantation material and a local focus of inflammation; (d) a compact plate with dilated Haversian canals and dilated full-blooded microvessels. Paraffin section. Stained with hematoxylin and eosin. Magnification 100 (a), magnification 400 (b–d)

In the NPC group, the histomorphological study revealed the formation of fibrous tissue with a layer of bone trabeculae on the outside at the border with the implant along its perimeter (Fig. 3 a). The connective tissue showed scarce cellularity, represented by a few fibroblastic differon cells and clusters of inflammatory cells (leukocytes, lymphocytes, plasma cells, monocyte-macrophage differon cells). Closer to the compact plate, fibrosing bone marrow with foci of inflammatory infiltrates was noted. Microvessels were few in number, mostly with fibrosed walls and obliterated lumens (Fig. 3 a). Imbibition of particles of the implantation material in the tissue of the peri-implantation area was noted (Fig. 3 b). Bone trabeculae of lamellar structure on the surface of the connective tissue sleeve had signs of chronic inflammation (Fig. 3 c). Haversian canals of the compact plate were unevenly expanded, mostly empty or filled with fibrous tissue (Fig. 3 d). Expressed osteoclastic resorption was not observed, the histological picture was probably associated with impaired bone microcirculation and the state of the chronic inflammatory process. According to the results of the morphometric study, the relative extent of the osteoblast surface was 57.2 %, the relative extent of the osteoclast surface was 1.7 %.

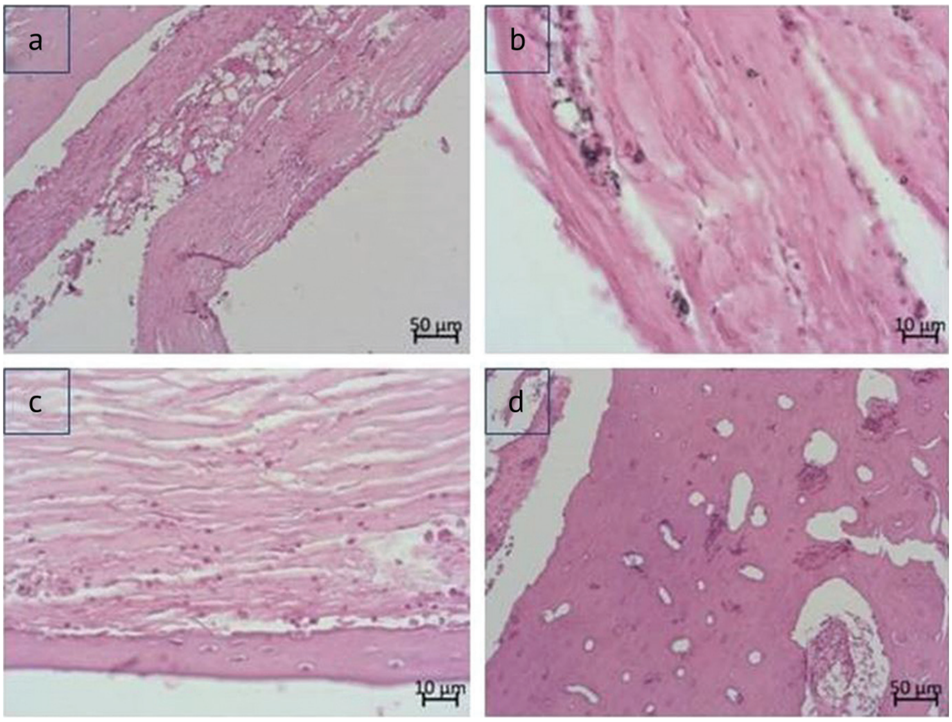

Fig. 3 Histological structure of tissues in the area of implantation of the NPC rod made: (a) formation of a fibrous sleeve with a thin trabecular layer outside around the implant, the bone marrow is fibrotic with foci of inflammatory infiltrate; (b) fibrous, poorly vascularized tissue adjacent to the implant, particles of the implantation material integrated into the connective tissue are visible; (c) bone trabeculae of a lamellar structure on the surface of the connective tissue case with signs of chronic inflammation; (d) compact plate with unevenly expanded, deserted, fibrotic Haversian canals. Paraffin section. Stained with hematoxylin and eosin. Magnification 100 (a, d); magnification 400 (b, c)

In the PC group, the results of histomorphological studies of implant osseointegration revealed that a layer of trabecular bone tissue was formed around the implant; its bone trabeculae were represented by reticulofibrous bone tissue, but closer to the compact plate the bone tissue had a lamellar structure;imbibition of material particles in the tissue of the peri-implantation area was revealed (Fig. 4 a, b). Between the compact plate and the bone tissue formed on the surface of the implant, gelatinous bone marrow with fatty inclusions and areas of hematopoiesis, or hematopoietic fatty bone marrow, were visualized. The bone marrow vessels had thin walls, were dilated and filled with blood cells and plasma, unevenly distributed in the vessel bed. On the surface of the bone trabeculae, consisting of lamellar bone tissue, functionally active osteoblasts located in a single row were more often visualized (Fig. 4 c). An active process of osteogenesis was noted on the surface and in the outer areas of the reticulofibrous bone trabeculae. Osteoclasts were rare and were often not attached to the surface of the trabeculae. However, resorption lacunae were found, filled with loose fibrous connective tissue with foci of osteogenesis or bone cells with newly formed amorphous bone substance in the pericellular space. The compact plate was characterized by widening of the lumens of some Haversian canals. On the periosteum side, foci of osteoclastic resorption were noted (Fig. 4 d). Morphometry showed that the relative extent of the osteoblast surface was 62.3 %, the relative extent of the osteoclast surface was 2.9 %. Thus, the new porous zirconium-based ceramics showed good osseointegration of the implant; the material used did not cause a pronounced negative impact on the tissues of the compact plate and bone marrow.

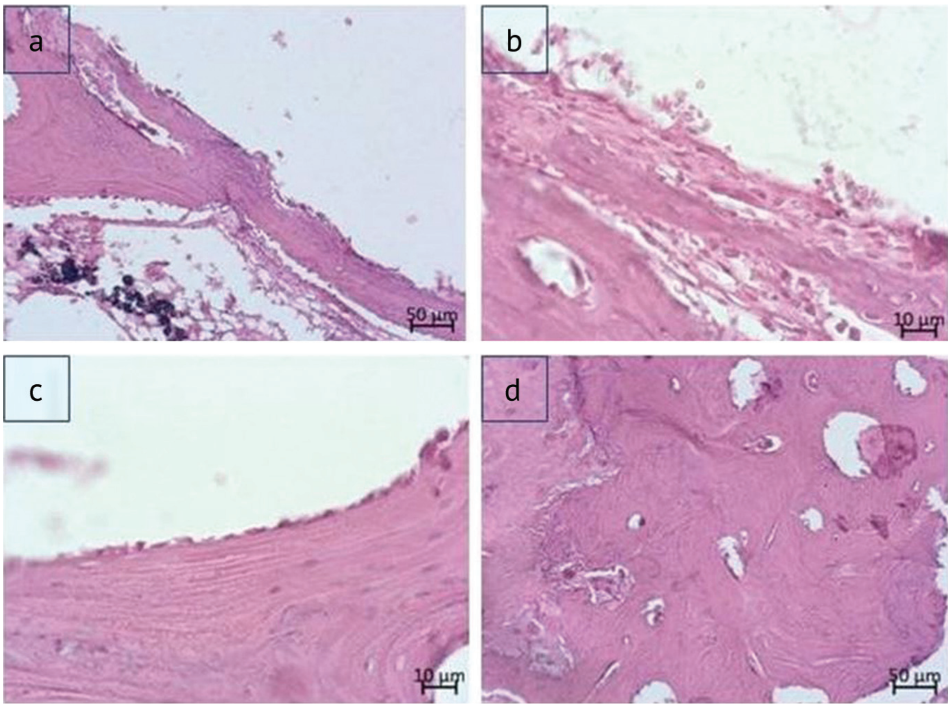

Fig. 4 Peculiarities of the histological structure of tissues in the area of implantation of a PC rod: (a) formation of a bone "sleeve" of trabecular structure around the implant, the space between newly formed bone trabeculae and the compact plate of the maternal bone is filled with hematopoietic fatty bone marrow with small areas of loose fibrous connective tissue; accumulations of particles of implanted material were found on the surface of bone trabeculae and in the intertrabecular spaces; (b) trabeculae of reticulo-fibrous bone tissue on the surface of the implant; (c) a layer of cuboid-shaped active osteoblasts on the surface of the bone trabeculae adjacent to the implant; (d) a compact plate with widened Haversian canals, enhanced adhesion lines and resorption from the periosteum. Paraffin section. Stained with hematoxylin and eosin. Magnification: 100 (a, d), magnification: 400 (b, c)

The results of histomorphological studies to determine the thickness of bone trabeculae in the implantation area in the TA, NPC and PC groups are presented in Figure 5. This indicator for the implanted porous ceramic rod was significantly higher not only compared to a titanium alloy implant ($p < 0.001$), but also compared to a non-porous ceramic implant ($p < 0.001$): 86.2 [55.8; 109.9] µm, 56.0 [47.2; 75.9] µm and 33.1 [19.0; 84.5] µm, respectively.

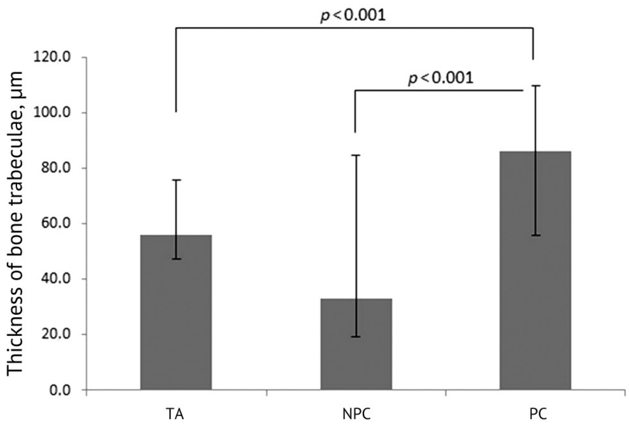

Fig. 5 Thickness of bone trabeculae in the area of implantation: titanium alloy (TA) rod, non-porous new ceramic material (NPC) and porous new ceramic material (PC) in rabbits

DISCUSSION

Due to the increase in human life expectancy and the aging of the population, the development of new materials and technologies for the functional replacement of a part of an organ or system is one of the key areas of scientific and technological strategy in the Russian Federation (Decree of the President of the Russian Federation No. 642). Special durable materials and structures with high osteointegrative characteristics are required, which will allow not only to recover the shape of the lost bone fragment, but also to restore the supporting function of the limb as a whole [15]. Ceramic materials as bone substitutes occupy a special place due to their unique combination of properties. High strength, wear resistance, low friction coefficient allow the use of such material under high loads, and compatibility with human tissues reduces the risk of inflammation and adverse reactions [16]. Moreover, the composition of the ceramic material can be adapted to improve specific properties [17]. To improve the biological and physical efficiency of multifunctional biomaterials, metal ions are used [18]; in particular, research is being conducted on alloying ceramics with rare earth elements [19]. Such alloy ceramic materials are attractive for tissue regeneration due to their functional properties, biological activity and therapeutic effects provided by the introduced ions [20].

In our experimental study, we investigated the biocompatibility and osseointegration of implants made of a new ceramic material based on zirconium oxide containing yttrium, ytterbium, and gadolinium ions. It has been previously proven that the introduction of zirconium into the composition of ceramics significantly improves the mechanical properties of materials [21]. At the same time, the presence of zirconium in composites does not have a cytotoxic effect on pre-osteoblasts [22], improves the reaction of osteoblasts in vitro [11], and does not affect the dynamics of hematological parameters [23]. Good results were obtained in clinical studies on the use of zirconium oxide implants [24]. The introduction of yttrium into zirconium dioxide-based ceramics provides exceptional mechanical properties; such a material demonstrates cytocompatibility and does not cause cytotoxic side-effects or allergic reactions in surrounding tissues [25]. The inclusion of ytterbium and gadolinium in the ceramic material promotes the proliferation and differentiation of mesenchymal stem cells of the bone marrow, stimulates the deposition of newly formed bone and collagen, and increases the durability of the ceramics [26, 27].

We conducted a study of the reaction of the experimental animal organism to the implantation of a new ceramic material based on zirconium oxide containing ions of yttrium, ytterbium, and gadolinium. We obtained the main hematological indices in this experiment to fill diaphyseal bone tissue defects. Our study showed a similar reaction of the animal organism to the new material and the titanium alloy.

It is known that by changing the nature of the surface and porosity of the implant, its functional properties can be significantly changed. Thus, smaller pore sizes can increase molecular transport and removal of cellular metabolic waste. Conversely, large pore sizes promote cell movement [28, 29]. In our study, implants made of a new ceramic material are presented in two versions, non-porous and porous (with a pore size of 10–50 μm). It was determined that in the case of using non-porous ceramic samples and titanium alloy implants, the parameters of the leukocyte, erythrocyte and platelet blood components in the postoperative period do not have significant differences. Whereas in porous ceramics application, the level of leukocytes, the number of granulocytes and monocytes was lower than in the other two groups, which may indicate a less pronounced inflammatory process in response to the implantation of an artificial bone substitution material.

The results of previous studies prove that new bone actively forms in contact with zirconium ceramic surfaces; secreting osteoblasts are found peri-implant in large quantities [30]. Comparative studies have established that zirconium dioxide implants and titanium-based implants demonstrate similar results in terms of osseointegration indices [31, 32]. The results of our histomorphological studies have shown that the implanted rods made of porous zirconium ceramics show better integration compared to the titanium implants and the implants made of non-porous zirconium ceramics.

Titanium and non-porous ceramic rods showed moderate or insignificant osseointegration. Moreover, signs of chronic inflammation were noted, which indicated a worse survival rate of these implants.

CONCLUSION

The development of new bioceramics based on zirconium oxide and containing ions of yttrium, ytterbium, gadolinium for compensation of bone and osteoarticular critical size defects is grounded on the physical and chemical stability, high mechanical strength of the material, the possibility of demonstrating not only osteoconductive, but also osteoinductive properties. The biological compatibility of the new ceramic material for filling diaphyseal defects of bone tissue was established in an experiment on animals. Implants with pore sizes of 10–50 μm have good osteointegrative characteristics, which determines the possibility and necessity of conducting clinical trials (with the permission of Roszdravnadzor).

Conflict of interests *None.*

Ethical approval *The study was approved by the institutional ethics board of the Ural State Medical University, protocol dated 05.20.2020 No. 5.*

REFERENCES

1. *Healthcare in Russia. 2021: Stat.sb./Rosstat*. Moscow; 2021:171. Available at: https://youthlib.mirea.ru/ru/reader/1357. Accessed Mar 18, 2025. (In Russ.)
2. Krivenko SN, Shpachenko NN, Popov SV. Emergency medical care at the prehospital stage and outcome prediction for concomitant injuries with spine-and-spinal cord trauma as their component. *Genij Ortopedii*. 2015;(3):22-25. (In Russ.) https://doi.org/10.18019/1028-4427-2015-3-22-25.
3. Tsiskarashvili AV, Zhadin AV, Kuzmenkov KA, et al. Biomechanically validated transosseus fixation in patients with femur pseudarthrosis complicated by chronic osteomyelitis. *N.N. Priorov Journal of Traumatology and Orthopedics*. 2018;(3-4):71-78. (In Russ.) doi: 10.17116/vto201803-04171.
4. Borzunov DYu, Mokhovikov DS, Kolchin SN, et al. Problems and successes in the combined application of the Ilizarov and Masquelet technologies. *Genij Ortopedii*, 2022;28(5):652-658. doi: 10.18019/1028-4427-2022-28-5-652-658.
5. Mukhametov UF, Lyulin SV, Borzunov DY, et al. Alloplastic and Implant Materials for Bone Grafting: a Literature Review. *Creative surgery and oncology*. 2021;11(4):343-353. (In Russ.) doi: 10.24060/2076-3093-2021-11-4-343-353.
6. Volokitina EA, Antropova IP, Timofeev KA, Trufanenko RA. Current state and perspectives on the use of zirconium ceramic implants in traumatology and orthopaedics. *Genij Ortopedii*. 2024;30(1):114-123. doi: 10.18019/1028-4427-2024-30-1-114-123.
7. Archunan MW, Petronis S. Bone Grafts in Trauma and Orthopaedics. *Cureus*. 2021;13(9):e17705. doi: 10.7759/cureus.17705.
8. Rodríguez-Merchán EC. Bone Healing Materials in the Treatment of Recalcitrant Nonunions and Bone Defects. *Int J Mol Sci*. 2022;23(6):3352. doi: 10.3390/ijms23063352.
9. Bohner M, Santoni BLG, Döbelin N. β-tricalcium phosphate for bone substitution: Synthesis and properties. *Acta Biomater*. 2020;113:23-41. doi: 10.1016/j.actbio.2020.06.022.
10. Padhye NM, Calciolari E, Zuercher AN, et al. Survival and success of zirconia compared with titanium implants: a systematic review and meta-analysis. *Clin Oral Investig*. 2023;27(11):6279-6290. doi: 10.1007/s00784-023-05242-5.
11. Chen Y, Roohani-Esfahani SI, Lu Z, et al. Zirconium ions up-regulate the BMP/SMAD signaling pathway and promote the proliferation and differentiation of human osteoblasts. *PLoS One*. 2015;10(1):e0113426. doi: 10.1371/journal.pone.0113426.
12. Tarasova N, Galisheva A, Belova K, et al. Ceramic materials based on lanthanum zirconate for the bone augmentation purposes: materials science approach. *Chimica Techno Acta*. 2022;9(2):09. doi: 10.15826/chimtech.2022.9.2.09.
13. Willbold E, Gu X, Albert D, et al. Effect of the addition of low rare earth elements (lanthanum, neodymium, cerium) on the biodegradation and biocompatibility of magnesium. *Acta Biomater*. 2015;11:554-562. doi: 10.1016/j.actbio.2014.09.041.
14. Jiang C, Shang J, Li Z, et al. Lanthanum Chloride Attenuates Osteoclast Formation and Function Via the Downregulation of Rankl-Induced Nf-κb and Nfatc1 Activities. *J Cell Physiol*. 2016;231(1):142-151. doi: 10.1002/jcp.25065.
15. Niu Y, Du T, Liu Y. Biomechanical Characteristics and Analysis Approaches of Bone and Bone Substitute Materials. *J Funct Biomater*. 2023;14(4):212. doi: 10.3390/jfb14040212.
16. Kaur G, Kumar V, Baino F, et al. Mechanical properties of bioactive glasses, ceramics, glass-ceramics and composites: State-of-the-art review and future challenges. *Mater Sci Eng C Mater Biol Appl*. 2019;104:109895. doi: 10.1016/j.msec.2019.109895.
17. Vaiani L, Boccaccio A, Uva AE, et al. Ceramic Materials for Biomedical Applications: An Overview on Properties and Fabrication Processes. *J Funct Biomater*. 2023;14(3):146. doi: 10.3390/jfb14030146.
18. Bai L, Song P, Su J. Bioactive elements manipulate bone regeneration. *Biomater Transl*. 2023;4(4):248-269. doi: 10.12336/biomatertransl.2023.04.005.

19. Chen Z, Zhou X, Mo M, et al. Systematic review of the osteogenic effect of rare earth nanomaterials and the underlying mechanisms. *J Nanobiotechnology*. 2024;22(1):185. doi: 10.1186/s12951-024-02442-3.
20. Li H, Xia P, Pan S, et al. The Advances of Ceria Nanoparticles for Biomedical Applications in Orthopaedics. *Int J Nanomedicine*. 2020;15:7199-7214. doi: 10.2147/IJN.S270229.
21. Izmodenova MYu, Gilev MV, Ananyev MV, et al. Bone Tissue Properties after Lanthanum Zirconate Ceramics Implantation: Experimental Study. *Traumatology and Orthopedics of Russia*. 2020;26(3):130-140. doi: 10.21823/2311-2905-2020-26-3-130-140.
22. Bhowmick A, Pramanik N, Jana P, et al. Development of bone-like zirconium oxide nanoceramic modified chitosan based porous nanocomposites for biomedical application. *Int J Biol Macromol*. 2017;95:348-356. doi: 10.1016/j.ijbiomac.2016.11.052.
23. Antropova IP, Volokitina EA, Udintseva MYu, et al. Effect of Lanthanum Zirconate Ceramic on the Dynamics of Hematological Parameters and the Bone Remodeling Markers:Experimental Study. *Traumatology and Orthopedics of Russia*. 2022;28(1):79-88. (In Russ.). doi: 10.17816/2311-2905-1704.
24. Mohseni P, Soufi A, Chrcanovic BR. Clinical outcomes of zirconia implants: a systematic review and meta-analysis. *Clin Oral Investig*. 2023;28(1):15. doi: 10.1007/s00784-023-05401-8.
25. Pantulap U, Arango-Ospina M, Boccaccini AR. Bioactive glasses incorporating less-common ions to improve biological and physical properties. *J Mater Sci Mater Med*. 2021;33(1):3. doi: 10.1007/s10856-021-06626-3.
26. Liao F, Peng XY, Yang F, et al. Gadolinium-doped mesoporous calcium silicate/chitosan scaffolds enhanced bone regeneration ability. *Mater Sci Eng C Mater Biol Appl*. 2019;104:109999. doi: 10.1016/j.msec.2019.109999.
27. Zhu DY, Lu B, Yin JH, et al. Gadolinium-doped bioglass scaffolds promote osteogenic differentiation of hBMSC via the Akt/GSK3β pathway and facilitate bone repair in vivo. *Int J Nanomedicine*. 2019;14:1085-1100. doi: 10.2147/IJN.S193576.
28. Wang Z, Zhang M, Liu Z, et al. Biomimetic design strategy of complex porous structure based on 3D printing Ti-6Al-4V scaffolds for enhanced osseointegration. *Mater. Des*. 2022;218:110721. doi: 10.1016/j.matdes.2022.110721.
29. Jin HW, Noumbissi S, Wiedemann TG. Comparison of Zirconia Implant Surface Modifications for Optimal Osseointegration. *J Funct Biomater*. 2024;15(4):91. doi: 10.3390/jfb15040091.
30. Scarano A, Di Carlo F, Quaranta M, Piattelli A. Bone response to zirconia ceramic implants: an experimental study in rabbits. *J Oral Implantol*. 2003;29(1):8-12. doi: 10.1563/1548-1336(2003)029<0008:BRTZCI>2.3.CO;2.
31. Gahlert M, Roehling S, Sprecher CM, et al. In vivo performance of zirconia and titanium implants: a histomorphometric study in mini pig maxillae. *Clin Oral Implants Res*. 2012;23(3):281-286. doi: 10.1111/j.1600-0501.2011.02157.x.
32. Kohal RJ, Weng D, Bächle M, Strub JR. Loaded custom-made zirconia and titanium implants show similar osseointegration: an animal experiment. *J Periodontol*. 2004;75(9):1262-1268. doi: 10.1902/jop.2004.75.9.1262.

The article was submitted 18.02.2025; approved after reviewing 14.03.2025; accepted for publication 31.03.2025.

Information about the authors:

Elena A. Volokitina — Doctor of Medical Sciences, Professor, Head of the Department,
volokitina_elena@rambler.ru, https://orcid.org/0000-0001-5994-8558;

Maksim V. Saushkin — assistant, saushkin66@mail.ru;

Irina P. Antropova — Doctor of Biological Sciences, Leading Researcher,
aip.hemolab@mail.ru, https://orcid.org/0000-0002-9957-2505;

Sergey M. Kutepov — Corresponding Member of the Russian Academy of Sciences, Doctor of Medical Sciences, Professor, Chief Researcher, kcm@usma.ru, https://orcid.org/0000-0002-3069-8150;

Svetlana A. Brilliant — Candidate of Biological Sciences, Researcher,
svetlana.brilliant@bk.ru, https://orcid.org/0000-0001-8640-6674.